

Optimistic DRX for Machine-type Communications

Hui-Ling Chang, Shang-Lin Lu, Tsung-Hui Chuang,

Chia-Ying Lin, Meng-Hsun Tsai

Department of Computer Science and Information Engineering

National Cheng Kung University, Taiwan, R.O.C.

Email: {p78041104,p76034509}@ncku.edu.tw,

{huei,a711186,tsaimh}@imslab.csie.ncku.edu.tw

Sok-Ian Sou

Institute of Computer and Communication Engineering

National Cheng Kung University, Taiwan, R.O.C.

Email: sisou@mail.ncku.edu.tw

Abstract—In Long Term Evolution-Advanced (LTE-A) network, Machine Type Communications (MTC) allows machines to transfer data with almost no human intervention. In MTC, power saving is one of the most important issues. In the meantime, the 3rd Generation Partnership Project (3GPP) proposes Discontinuous Reception (DRX) mechanism to allow user equipments (UEs) to receive data only at specified time slots and turn off the radio module at other time slots. Unfortunately, current DRX mechanism is designed for normal usage of mobile users, not for MTC. In this paper, we propose Optimistic DRX (ODRX) mechanism to allow more sleep periods for MTC devices. To allow more sleep periods, ODRX considers to release the RRC connection and re-establish the connection when the MTC device is paged. We propose analytical and simulation models for ODRX, and compare with the standard DRX through simulation experiments. The results show that, compared to standard DRX, significant extra power can be saved by sacrificing little extra wake up latency.

I. INTRODUCTION

Long Term Evolution-Advanced (LTE-Advanced), proposed by the Third Generation Partnership Project (3GPP), is the most promising fourth generation mobile network. In LTE-Advanced network, the 3GPP proposes Machine-type Communications (MTC) as a new paradigm where devices transfer data among themselves with limited human interaction. MTC is now widely used in many aspects, such as monitoring system and industrial automation. In most situations, devices keep silent until there are data delivered from/to them. However, if devices are active all the time, most of the power is wasted. In addition, many MTC devices are powered by battery. Certainly, power saving has already become an important issue in MTC.

In the meantime, the 3GPP proposes a power-saving mechanism, called Discontinuous Reception (DRX), to allow user equipments (UEs) to receive data only at specified time slots and turn off the radio module at other time slots. When DRX mode is turned on in a UE, Inactivity Timer is started. If some data arrive at the UE, the timer is re-started. Once the timer is expired (i.e., no data arrival during countdown of the timer), the UE enters a DRX cycle. In the DRX cycle, the UE monitors Physical Downlink Control Channel (PDCCH) only in the period called On Duration. In On Duration, if some data need to be received, the UE enters active mode, receives the data and re-starts Inactivity Timer.

Unfortunately, current DRX mechanism is designed for normal usage of mobile users, not for MTC. For a mobile user, latency is usually more important than power saving. However, in many cases, latency is not that important for an MTC application. In this paper, we propose an Optimistic DRX (ODRX) mechanism to allow more sleep periods for MTC devices. To allow more sleep periods, ODRX considers to release the Radio Resource Control (RRC) connection and re-establish the connection when the MTC device is paged. In other words, ODRX allows latency incurred from re-establishment of RRC connection as long as more power could be saved. To investigate performance of ODRX, we propose analytical and simulation models for ODRX, and compare with the standard DRX through simulation experiments.

This paper is organized as follows. Related works are described in section II. Section III introduces ODRX. In section IV, we present an analytical model to investigate performance of ODRX. Then we present a simulation model in section V to validate against the analytical model. Based on the validated simulation model, we investigate performance of ODRX in section VI. Finally, we conclude this paper in section VII.

II. RELATED WORK

In this section, we first describe existing works on DRX for normal usage. Then we discuss several works on DRX for MTC application.

The basic DRX modes and parameters in LTE are clearly introduced in [1]. In [2], the authors quantitatively analyze the effects of the inactivity timer threshold and the DRX cycle in UMTS. In [3], Yang proposes an algorithm to dynamically adjust inactivity timer and DRX cycle. These works focus on normal usage of mobile users, and are not able to be used directly for MTC application.

In MTC, packet sizes are assumed to be much smaller than usual and delivery time interval is assumed to be much longer. Based on these characteristics, DRX mechanism are re-investigated for MTC application in [4] and [5]. Effects of DRX parameters on wake-up latency and power saving factor are studied through semi-Markov chain. The results show that appropriate settings of DRX parameters are quite important in MTC application.

In [6], a QoS-aware DRX mechanism is proposed to meet QoS requirement on traffic bit-rate, packet delay and packet

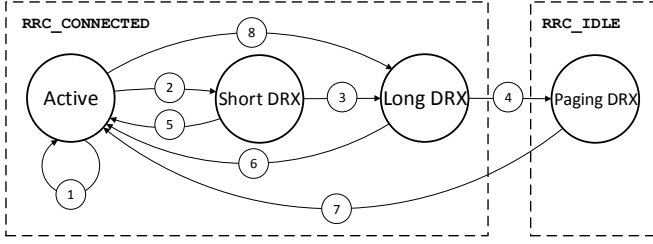


Fig. 1. Finite state machine of ODRX

loss rate. This method sacrifices a few power savings for achieving QoS requirement. However, in many MTC applications, power saving is much more important than QoS requirement as long as MTC devices are powered by battery. In this paper, we propose an optimistic DRX mechanism to save more energy for MTC application with slight or without QoS requirement.

III. OPTIMISTIC DRX

In this section, we introduce Optimistic DRX (ODRX) mechanism for MTC application.

The finite state machine of the ODRX mechanism in an MTC device is drawn in Fig. 1. Initially, the MTC device is at **Active** state, and the *Inactivity Timer* is started. A flag called *optimistic flag* is set to Off. The device at **Active** state keeps monitoring PDCCH continuously. If the device receives data from network before the Inactivity Timer expires, the device stays at **Active** state, restarts the timer, and sets the optimistic flag to Off (Path 1). Once the Inactivity Timer expires, the optimistic flag is checked. If the flag is Off, the device enters **Short DRX** state and starts *DRX Short Cycle Timer* (Path 2). Otherwise, the device enters **Long DRX** state and starts *DRX Long Cycle Timer* (Path 8). At the **Short DRX** state, the device monitors PDCCH only in On Duration period and then goes to sleep for a period (called Opportunity for DRX). If the device observes data in On Duration, the device returns to **Active** state (Path 5). When the DRX Short Cycle Timer expires, the device enters **Long DRX** state and starts DRX Long Cycle Timer (Path 3). The device's behavior at **Long DRX** state is basically the same as that at **Short DRX** state except that Opportunity for DRX in **Long DRX** state is longer. If the device observes data in On Duration, the device returns to **Active** state, and the optimistic flag is set to On (Path 6). When the DRX Long Cycle Timer expires, the device releases the radio resource and enters **Paging DRX** state (Path 4). In **Paging DRX** state, the device monitors PDCCH for a single subframe in each paging cycle. The eNB may page the device at the subframe if some data arrive at the eNB before the subframe. If the device is paged at the subframe, the device returns to **Active** state, and the optimistic flag is set to On (Path 7).

The major “optimistic” parts include (1) the adoption of **Paging DRX** state, and (2) the usage of optimistic flag. In **Paging DRX** state, if there is no data delivered to/from the device for a long time, the resource (i.e., the RRC connection) is not occupied and the device can save more power without

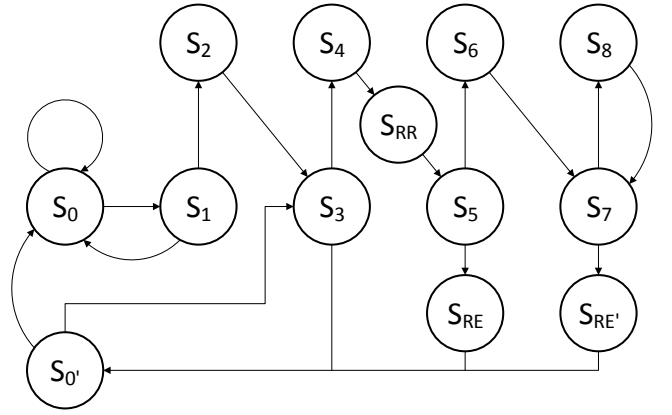


Fig. 2. semi-Markov chain for ODRX

RRC connection. Moreover, if the device comes back to **Active** state from **Long DRX** or **Paging DRX** state (Path 6 or 7), next time when the Inactivity Timer expires, the device enters **Long DRX** state directly instead of **Short DRX** (Path 8). Since many MTC applications incur small data transmission, skipping **Short DRX** state is more battery-efficient.

It is assumed that data transmission is intensive if data continuously arrive at the eNB. In this case, even if the device just returns back from **Long DRX** or **Paging DRX** state, the optimistic flag is set to off by the consecutive data packet (Path 1). Then the device enters **Short DRX** instead of **Long DRX** when the Inactivity Timer expires for the next time.

IV. ANALYTICAL MODEL

In this section, we propose an analytical model to provide estimate of power saving factor and wake up latency of our method. Fig. 2 illustrates a semi-Markov chain for ODRX.

In the semi-Markov chain, state S_0 and S_0' denote **Active** with *optimistic flag*=0 and *optimistic flag*=1, respectively. States S_1 and S_2 denote the On Duration and the Opportunity period respectively in **Short DRX**. States S_3 and S_4 denote the On Duration and the Opportunity period respectively in **Long DRX**. States S_5 , S_6 , S_7 and S_8 denote **Paging DRX**. MTC device monitors PDCCH at states S_5 and S_7 , and sleeps at states S_6 and S_8 . State S_{RR} denotes that the RRC connection is being released. States S_{RE} and $S_{RE'}$ denote that an RRC connection is being established. Note that state holding times of states S_{RR} , S_{RE} and $S_{RE'}$ are used to estimate extra latency incurred in RRC connection establishment and release.

Table I shows the notations used in analytical model. We first derive the stationary probabilities π_i in subsection IV-A. Then we derive the state holding times H_i in subsection IV-B. Based on the derived stationary probabilities and state holding times, we derive the power saving factor α and the wake up latency δ in subsection IV-C.

A. Stationary Probability

Denote $p_{i,j}$ as the transition probability from S_i to S_j and π_i as the stationary probability of state S_i . The stationary

TABLE I
NOTATIONS USED IN ANALYTICAL MODEL

π_i	stationary probability at S_i
H_i	state holding time at S_i
α	power saving factor
δ	wake up latency
$p_{i,j}$	transition probability from S_i to S_j
t_p	inter-packet arrival time
T_0	Inactivity Timer
T_{ON}	On Duration Timer
T_{sub}	length of a subframe (1 ms)
T_S	Short Cycle Timer
T_L	Long Cycle Timer
T_I	Paging Cycle Timer
T_{RR}	latency of RRC connection release
T_{RE}	latency of RRC connection establishment
P_{sd}	sleeping ratio in DRX short cycle
P_{ls}	sleeping ratio in DRX long cycle
P_{id}	sleeping ratio in paging cycle
T	average system time

probabilities are expressed as:

$$\begin{aligned}
\pi_j &= \pi_{j-1} \cdot p_{j-1,j}, \quad j = 1, 2, 4, 6, 8 \\
\pi_{RR} &= \pi_4 \cdot p_{4,RR}, \\
\pi_5 &= \pi_{RR} \cdot p_{RR,5}, \\
\pi_7 &= \pi_6 \cdot p_{6,7} + \pi_8 \cdot p_{8,7}, \\
\pi_{RE} &= \pi_5 \cdot p_{5,RE}, \\
\pi_{RE'} &= \pi_7 \cdot p_{7,RE'}, \\
\pi_{0'} &= \pi_3 \cdot p_{3,0'} + \pi_{RE} \cdot p_{RE,0'} + \pi_{RE'} \cdot p_{RE',0'}, \\
\pi_0 &= \pi_{0'} \cdot p_{0',0} + \pi_0 \cdot p_{0,0} + \pi_1 \cdot p_{1,0}. \quad (1)
\end{aligned}$$

Assume that packet arrivals form a Poisson process with parameter λ , thus the inter-arrival time t_p of packets follows exponential distribution with mean $1/\lambda$. Based on the characteristics of MTC application, we assume that there is at most one packet arrival during a short/long/paging cycle. This limitation is relaxed in simulation experiments.

Denote T_0 as the Inactivity Timer. If no data packet arrives before T_0 expires at S_0 state, transition from S_0 to S_1 occurs. In this case, the state transition probability $p_{0,1}$ is expressed as

$$p_{0,1} = \Pr(t_p > T_0) = e^{-\lambda T_0}. \quad (2)$$

Denote T_{ON} as the On Duration Timer, T_{sub} as length of a subframe, T_S as Short Cycle Timer, T_L as Long Cycle Timer, and T_I as Paging Cycle Timer. For an RRC connection, let T_{RR} be the latency of RRC connection release, and T_{RE} be the latency of RRC connection establishment. Similarly,

$$\begin{aligned}
p_{1,2} &= \Pr(t_p > T_{ON}) = e^{-\lambda T_{ON}}, \\
p_{5,6} &= \Pr(t_p > (T_L - T_{ON} + T_{RR} + T_{sub})) \\
&= e^{-\lambda(T_L - T_{ON} + T_{RR} + T_{sub})}, \\
p_{7,8} &= \Pr(t_p > T_I) = e^{-\lambda T_I}, \\
p_{0',3} &= \Pr(t_p > T_0) = e^{-\lambda T_0}. \quad (3)
\end{aligned}$$

On the other hand, if a packet arrives before T_0 expires at S_0 state, the device stays at S_0 . The transition probability $p_{0,0}$ is expressed as

$$p_{0,0} = \Pr(t_p < T_0) = 1 - e^{-\lambda T_0}. \quad (4)$$

Similarly,

$$\begin{aligned}
p_{1,0} &= \Pr(t_p < T_{ON}) = 1 - e^{-\lambda T_{ON}}, \\
p_{5,RE} &= \Pr(t_p < (T_L - T_{ON} + T_{RR} + T_{sub})) \\
&= 1 - e^{-\lambda(T_L - T_{ON} + T_{RR} + T_{sub})}, \\
p_{7,RE'} &= \Pr(t_p < T_I) = 1 - e^{-\lambda T_I}, \\
p_{0',0} &= \Pr(t_p < T_0) = 1 - e^{-\lambda T_0}. \quad (5)
\end{aligned}$$

When the device is at S_2 , the transition to S_3 certainly occurs. So $p_{2,3} = 1$. Similarly, $p_{4,RR} = p_{RR,5} = p_{6,7} = p_{8,7} = p_{RE,0'} = p_{RE',0'} = 1$.

Note that there are two cases for the transition from S_3 to S_4 : (i) the device comes from S_2 and transfers to S_4 with probability $p_{3,4}' = \Pr(t_p > T_S) = e^{-\lambda T_S}$; (ii) the device comes from $S_{0'}$ and transfers to S_4 with probability $p_{3,4}'' = \Pr(t_p > T_{ON}) = e^{-\lambda T_{ON}}$. In this case, we have to derive $p_{3,4}$ based on the ratio of $\pi_2 \cdot p_{2,3}$ and $\pi_{0'} \cdot p_{0',3}$ which is calculated as

$$(1 - e^{-\lambda T_0}) : e^{-\lambda T_0}. \quad (6)$$

By partial derivation of equations (1)-(5), we have

$$\begin{aligned}
p_{3,4} &= p_{3,4}' \cdot (1 - e^{-\lambda T_0}) + p_{3,4}'' \cdot e^{-\lambda T_0} \\
&= e^{-\lambda T_S} - e^{-\lambda(T_0 + T_S)} + e^{-\lambda(T_0 + T_{ON})}. \quad (7)
\end{aligned}$$

On the contrary,

$$p_{3,0'} = 1 - e^{-\lambda T_S} + e^{-\lambda(T_0 + T_S)} - e^{-\lambda(T_0 + T_{ON})}. \quad (8)$$

From $\sum_i \pi_i = 1$ and equations (1)-(7), we can easily obtain the stationary probabilities (the final equations are ignored here).

B. State Holding Time

In this subsection, we derive the state holding time H_i for each state. At S_0 , there are two cases for packet arrivals: (i) packet arrives before the expiry of T_0 ; (ii) packet arrives after the expiry of T_0 , so $H_0 = p_{0,1} \cdot T_0 + \sum_{i=1}^{T_0} p_i \cdot T_i$, where p_i is the probability that the packet arrive at the i th subframe and T_i is the holding time that the same case as above, so $p_i = \Pr(i-1 < t_p < i) = e^{-\lambda(i-1)} - e^{-\lambda i}$, $i \in [1, T_0]$ and $T_i = H_0 + i$. Therefore, we obtain

$$H_0 = \frac{1 - e^{-\lambda T_0}}{(1 - e^{-\lambda})e^{-\lambda T_0}}. \quad (9)$$

The calculation of $H_{0'}$ is similar to that of H_0 . The only difference is that $T_i = i$. So we can get

$$H_{0'} = \frac{1 - e^{-\lambda T_0}}{1 - e^{-\lambda}}. \quad (10)$$

Similarly,

$$H_1 = \frac{1 - e^{-\lambda T_{ON}}}{1 - e^{-\lambda}}. \quad (11)$$

H_2 is the sleep period of an UE during a short cycle, so $H_2 = T_S - T_{ON}$. Similarly, $H_4 = T_L - T_{ON}$, $H_{RR} = T_{RR}$, $H_6 = T_I - T_{sub}$, $H_8 = T_I - T_{sub}$, $H_{RE} = T_{RE}$ and $H_{RE'} = T_{RE}$.

At S_3 , we have to derive H_3 based on the ratio of $\pi_2 \cdot p_{2,3}$ and $\pi_{0'} \cdot p_{0',3}$, too. When the device comes from S_2 , there are three cases for the arrival of packets: (i) the packet arrive at the sleep period of last short cycle; (ii) the packet arrive before the expiry of T_{ON} ; (iii) the packet arrive after the expiry of T_{ON} , so $H_3 = p_S \cdot T_{sub} + \sum_{j=1}^{T_{ON}} p_j^{ON} \cdot T_j^{ON} + p_{3,4} \cdot T_{ON}$. p_S is the probability that case (i) occurs so $p_S = \Pr(t_p < T_S - T_{ON})$. T_{sub} is the subframe that UE takes to receive the packet from eNB so $T_{sub} = 1$. $p_j^{ON} = \Pr(T_S - T_{ON} + j - 1 < t_p < T_S - T_{ON} + j) = e^{-\lambda(T_S - T_{ON} + j - 1)} - e^{-\lambda(T_S - T_{ON} + j)}$, $j \in [1, T_{ON}]$ and $T_j^{ON} = j$, $j \in [1, T_{ON}]$. Hence, we can obtain

$$H_3' = \frac{e^{-\lambda(T_S - T_{ON})} - e^{-\lambda T_S}}{1 - e^{-\lambda}} + 1 - e^{-\lambda(T_S - T_{ON})}. \quad (12)$$

On the other hand, when the device comes from $S_{0'}$, we can derive another H_3 similarly. That is,

$$H_3'' = \frac{1 - e^{-\lambda T_{ON}}}{1 - e^{-\lambda}}. \quad (13)$$

Finally, we get actual H_3 by the equation bellow:

$$H_3 = H_3' \cdot (1 - e^{-\lambda T_0}) + H_3'' \cdot e^{-\lambda T_0}. \quad (14)$$

Note that at S_5 and S_7 , whenever the packet arrive, it takes T_{sub} staying in that state. If the packet arrive before or right at S_5 or S_7 , the UE takes T_{sub} monitoring the PDCCH to detect whether there is any packet to receive or not. On the other hand, if packet arrive after T_{sub} , the UE will go into sleep period of the DRX cycle (paging cycle). From the discussion above, we know that $H_5 = 1$ and $H_7 = 1$.

C. Power Saving Factor and Wake Up Latency

Denote T as the average system time, thus T is expressed as

$$T = \sum_{i=0}^8 \pi_i H_i + \pi_{RR} H_{RR} + \pi_{RE} H_{RE} + \pi_{RE'} H_{RE'} + \pi_{0'} H_{0'}. \quad (15)$$

Let α be the power saving factor and δ be the wake up latency. We define the power saving factor $\alpha = P_{sd} + P_{ld} + P_{id}$, where P_{sd} , P_{ld} and P_{id} are the ratios of the sleeping period to the average system time T , respectively. That is,

$$P_{sd} = \frac{\pi_2 H_2}{T}, \quad (16)$$

$$P_{ld} = \frac{\pi_4 H_4}{T}, \quad (17)$$

$$P_{id} = \frac{\pi_6 H_6 + \pi_8 H_8}{T}. \quad (18)$$

If the device is sleeping, wake up latency represents the interval between the packet arrival and the next On Duration. Otherwise, wake up latency is zero. Since the packet arrivals

TABLE II
SIMULATION VALIDATION

$1/\lambda$ (unit: s)	1	10	100	300
Analytical α	0.8837	0.9800	0.9965	0.9978
Simulation α	0.8625	0.9795	0.9965	0.9978
Error Rate	2.4%	0.05%	0%	0%
Analytical δ	330.7918	402.1955	414.5193	415.5058
Simulation δ	315.0393	401.8073	414.5189	415.5050
Error Rate	4.76%	0.97%	0%	0%

are random observers in each state, and each cycle time is fixed, from excess life theorem [7], we have

$$\begin{aligned} \delta = & P_{sd} \cdot \frac{T_S - T_{ON}}{2} + P_{ld} \cdot \frac{T_L - T_{ON}}{2} \\ & + \frac{\pi_{RR} H_{RR}}{T} \cdot \left(\frac{T_{RR}}{2} + T_{sub} + T_{RE} \right) \\ & + \frac{\pi_5 H_5 + \pi_7 H_7}{T} \cdot T_{RE} + P_{id} \cdot \left(\frac{T_I - T_{sub}}{2} + T_{sub} + T_{RE} \right) \\ & + \frac{\pi_{RE} H_{RE} + \pi_{RE'} H_{RE'}}{T} \cdot \frac{T_{RE}}{2}. \end{aligned} \quad (19)$$

Note that π_3 does not need to be calculated here because the equations for α and δ can be reduced by dividing the numerator and denominator by π_3 .

V. SIMULATION

In this section, a simulation model is constructed to validate against the analytical model. Fig. 3 illustrates a simplified simulation flow chart. Step 1 initializes the parameters. A packet p is generated as current packet with its arrival time stamp $p.arr = Poisson_interarr$, where $Poisson_interarr$ is exponentially distributed. A state s is also generated as current state with type $s.type = S_0$ and its termination time stamp $s.term = T_0$ (where T_0 is the Inactivity Timer). Step 2 checks the current state. Note that for each case, the accumulations of delay and holding time of the corresponding state are omitted in this figure.

If $s.type = S_0$, step 3 compares $s.term$ with $p.arr$. If $p.arr < s.term$ (i.e., the packet arrives before the Inactivity Timer expires), the device stays at S_0 ($s.type = S_0$), and Inactivity Timer is re-started by setting $s.term = p.arr + T_0$. If $p.arr \geq s.term$ at step 3, the device enters Short DRX state by setting $s.type = S_1$.

Steps 6-8, Steps 9-11 and Steps 12-14 are similar to Steps 3-5, and the details are ignored. Step 15 checks whether sufficient packet arrivals are processed.

Table II compares the analytical model and the simulation experiments with parameters $T_0 = 20ms$, $T_{ON} = 80ms$, $T_{sub} = 1ms$, $T_S = 160ms$, $T_L = 320ms$ and $T_I = 64$ radio frames (640ms). Note that $T_{RR} = 1ms$ and $T_{RE} = 97ms$ ($= T_{RE'}$) are assumed according to [8]. The table indicates that the analytical model and the simulation experiments are consistent when $1/\lambda > 1$. The inconsistency occurs when packet arrival rate is large. In this case, more than two packet

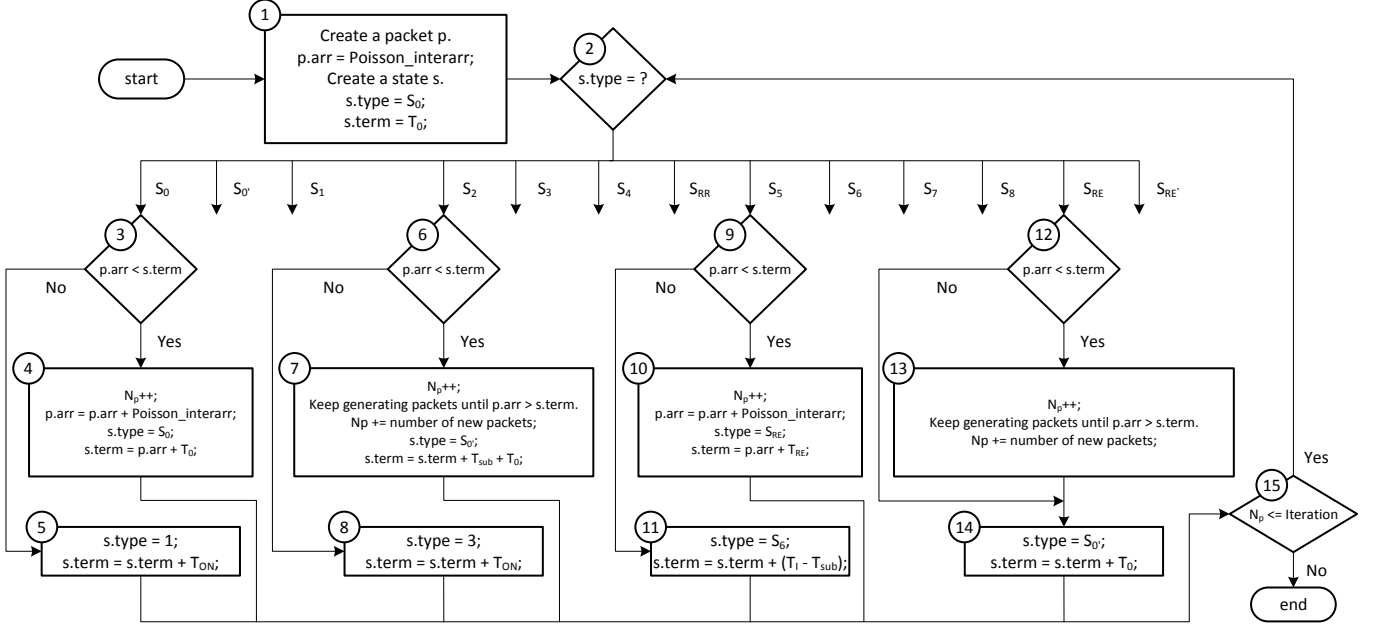


Fig. 3. Simulation Flow Chart

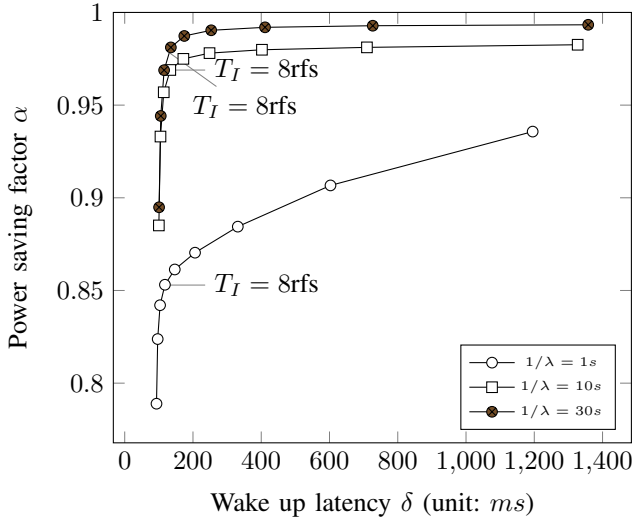


Fig. 4. Wake up latency and power saving factor under different $1/\lambda$ and T_I . $T_0 = 20ms$, $T_{ON} = 80ms$, $T_{sub} = 1ms$, $T_S = 160ms$, $T_L = 320ms$, $T_{RR} = 1ms$ and $T_{RE} = 97ms$

arrivals may be observed in a short/long/paging cycle in simulation experiments. Since we assume only single packet may arrive in a short/long/paging cycle, the inconsistency is acceptable.

VI. PERFORMANCE EVALUATION

Fig. 4 illustrates the relationship between δ and α under different $1/\lambda$ and T_I . T_I is set to 1, 2, 4, 8, 16, 32, 64, 128 and 256 radio frames respectively. We observe that α converges before $\delta = 200$ when $1/\lambda > 1s$ (corresponding T_I at the turning point is 8 radio frames). In principle, α

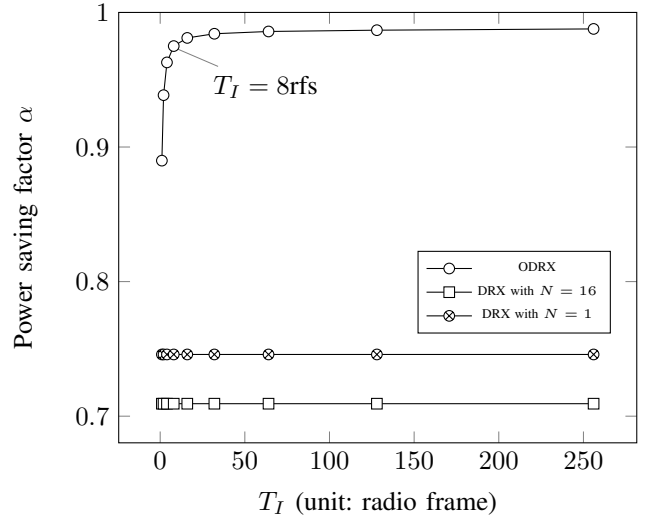


Fig. 5. Power saving factor comparison under different T_I ($1/\lambda = 15s$, $T_0 = 20ms$, $T_{ON} = 80ms$, $T_{sub} = 1ms$, $T_S = 160ms$, $T_L = 320ms$, $T_{RR} = 1ms$ and $T_{RE} = 97ms$)

and δ increases as T_I increases. However, we observe that α converges very quickly as T_I increases. On the other hand, δ increases linearly as T_I increases. The results show that $T_I = 8$ radio frames is sufficient to provide large power saving as well as sacrificing little wake up latency. Note that when $1/\lambda$ is small (e.g., $1/\lambda = 1s$), a large T_I is required to provide significant power saving. In MTC application, $1/\lambda$ is usually large. Therefore, we can easily find optimal setting (the turning point) for ODRX.

Fig. 5 and Fig. 6 compare ODRX and the standard DRX in terms of α and δ . Note that standard DRX does not have

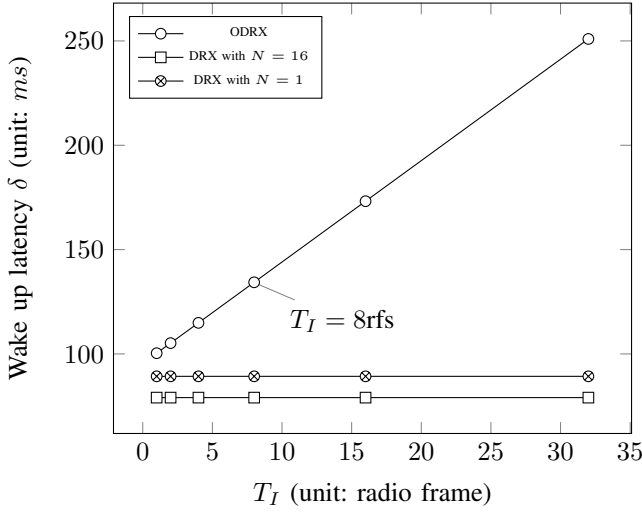


Fig. 6. Wake up latency comparison under different T_I ($1/\lambda = 15s$, $T_0 = 20ms$, $T_{ON} = 80ms$, $T_{sub} = 1ms$, $T_S = 160ms$, $T_L = 320ms$, $T_{RR} = 1ms$ and $T_{RE} = 97ms$)

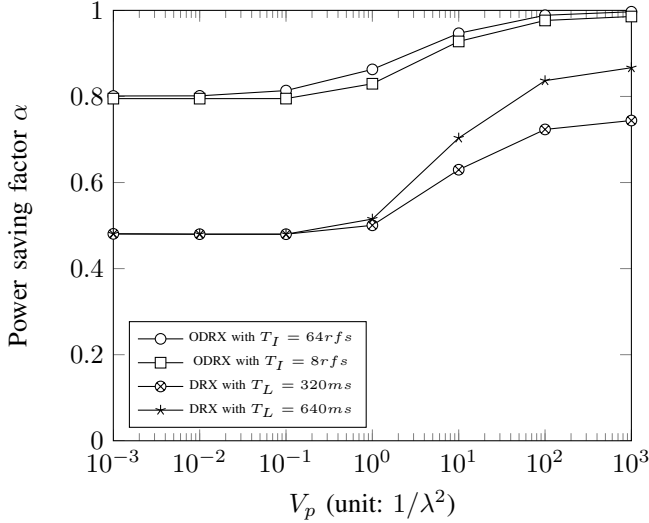


Fig. 7. Effects of V_p , T_L and T_I on power saving factor ($1/\lambda = 1000ms$, $T_0 = 20ms$, $T_{ON} = 80ms$, $T_{sub} = 1ms$, $T_S = 160ms$, $N = 16$, $T_{RR} = 1ms$ and $T_{RE} = 97ms$)

parameter T_I , thus the curve of DRX is horizontal. In Fig. 5, compared to standard DRX, significant improvement in terms of α is observed. In ODRX, much more power is saved in Paging DRX state. Fig. 6 shows intuitive results that δ increases linearly as T_I increases. When $T_I = 8$ radio frames and $N = 1$, extra 45ms (134ms - 89ms) of wake up latency is incurred. In the meantime, extra 23% (97% - 74%) of power saving is observed (see Fig. 5). Fortunately, in many MTC applications, 45ms of wake up latency can be ignored, but 23% of power saving is noticeable.

To observe adaptability of ODRX to more practical situations, assume that the inter-packet arrival time t_p is Gamma distributed with mean $1/\lambda$ and variance V_p . Fig. 7 shows the effect of V_p on α . In this figure, α for both ODRX and DRX increases as V_p increases. This phenomena is explained as

follows. As V_p increases, more short and long inter-packet intervals are observed. Packets arriving with short inter-packet intervals is bursty. These bursty packets are more likely to arrive in the same Active state. On the other hand, packets arriving with long inter-packet intervals are more likely to arrive in Paging DRX state. As a result, the MTC device stays much longer in Paging DRX state when V_p is large. In other words, more power is saved when the inter-packet arrival intervals become more irregular.

VII. CONCLUSION

In this paper, we proposed ODRX mechanism to allow more sleep periods for MTC devices. To allow more sleep periods, ODRX considers to release the RRC connection and re-establish the connection when the MTC device is paged. We proposed analytical and simulation models for ODRX, and compared with the standard DRX through simulation experiments. The results show that, compared to standard DRX, significant extra power can be saved by sacrificing little extra wake up latency. Furthermore, more power is saved when the inter-packet arrival intervals become more irregular.

ACKNOWLEDGMENT

M.-H. Tsai's work was sponsored in part by Ministry of Science and Technology (MOST), Taiwan, under the contract number MOST 104-2221-E-006-041- and MOST104-3115-E-009-006-. The work of S.-I. Sou was sponsored in part by MOST, Taiwan, under the contract number NSC 102-2221-E-006-112-MY3.

REFERENCES

- [1] C. Bontu and E. Illidge, "Drx mechanism for power saving in lte," *IEEE Communications Magazine*, vol. 47, no. 6, pp. 48–55, Jun. 2009.
- [2] S.-R. Yang and Y.-B. Lin, "Modeling umts discontinuous reception mechanism," *IEEE Transactions on Wireless Communications*, vol. 4, no. 1, pp. 312–319, Jan. 2005.
- [3] S.-R. Yang, "Dynamic power saving mechanism for 3g umts system," *Mobile Networks and Applications*, vol. 12, no. 1, pp. 5–14, 2007.
- [4] J. Wu, T. Zhang, Z. Zeng, and H. Chen, "Study on discontinuous reception modeling for m2m traffic in lte-a networks," in *In proceeding of the 15th IEEE International Conference on Communication Technology (ICCT)*, Nov. 2013.
- [5] K. Zhou, N. Nikaein, and T. Spyropoulos, "Lte/lte-a discontinuous reception modeling for machine type communications," *IEEE Wireless Communications Letters*, vol. 2, no. 1, pp. 102–105, Feb. 2013.
- [6] J.-M. Liang, J.-J. Chen, H.-H. Cheng, and Y.-C. Tseng, "An energy-efficient sleep scheduling with qos consideration in 3gpp lte-advanced networks for internet of things," *IEEE Journal on Emerging and Selected Topics in Circuits and Systems*, vol. 3, no. 1, pp. 13–22, Mar. 2013.
- [7] S. Ross, *Stochastic processes*. Wiley, 1996.
- [8] S. Mohan, R. Kapoor, and B. Mohanty, "Latency in hspa data networks," *Qualcomm, Tech. Rep.*, 2011.